JCTC Journal of Chemical Theory and Computation

Article

pubs.acs.org/JCTC

Many-Body Convergence of the Electrostatic Properties of Water

Gregory R. Medders and Francesco Paesani*

Department of Chemistry and Biochemistry, University of California, San Diego, La Jolla, California 92093, United States

Supporting Information

ABSTRACT: The many-body convergence of the dipole moment and the dipole−dipole polarizability of water is investigated. It is found that, for systems of low symmetry like the water clusters examined here, simple measures such as dipole magnitudes and average polarizabilities may lead to an incomplete interpretation of the underlying physics. Alternative metrics are introduced that allow for an unambiguous characterization of both properties. The convergence of the many-body decomposition of the total dipole and the polarizability is studied for $(H_2O)_N$, with $N = 4-6$ being minimum energy water clusters and $N = 14$ being clusters that were extracted from condensed phase simulations. For these clusters, it is demonstrated that both the total dipole and polarizability are almost entirely pairwise additive, with three-body terms contributing less than 4% and all higher-order terms being essentially negligible.

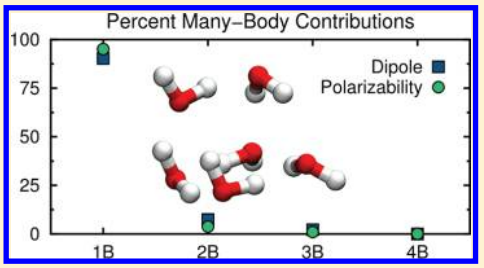

1. INTRODUCTION

Water is a key component of many chemical processes with important implications in fields as diverse as biology and geology. It is often found in crowded environments (e.g., living cells[1,2]) where it acts as a solvent for ionic species and biomolecules, at interfaces (e.g., environmental surfaces[3−5]) where it controls ion adsorption and dissolution, and in confined environments (e.g., proton-exchange membranes and metal−organic frameworks[6−8]). To a significant extent, the unique behavior of water may be attributed to its ability to establish a dense yet dynamic hydrogen-bond (HB) network.[9] In the past decade, linear and nonlinear vibrational spectroscopy has emerged as a powerful technique that, by complementing the existing scattering methodologies, can provide direct insights into the structure and dynamics of the water HB network in different environments. Within linear response theory, vibrational spectra, including infrared (IR), Raman, sum-frequency generation (SFG), and two-dimensional infrared (2D-IR) spectra, can be calculated from the Fourier transforms of appropriate single- or multitime correlation functions involving the system dipole and/or polarizability.[10] It thus follows that an accurate representation of both the dipole and polarizability of water is necessary for the calculation of vibrational spectra that can be directly compared with the corresponding experimental measurements. This, in turn, is key to the molecular-level characterization of the structural and dynamical properties of water in different environments and conditions.

As discussed in ref 11, a systematic analysis of the electrostatic properties of a molecular system begins by investigating the energy of a single molecule interacting at long-range with an external electric field F_α ($\alpha = x, y, z$). Up to the second-order perturbation in the electric field, the interaction is given by

$$E = E_0 - \mu_\alpha F_\alpha - \frac{1}{2} F_\alpha \alpha_{\alpha\beta} F_\beta \tag{1}$$

where terms involving derivatives of the electric field have been neglected and the repeated greek indices imply sums over the corresponding Cartesian coordinates. In eq 1, μ_α is the static, field-independent molecular dipole and $\alpha_{\alpha\beta}$ is the dipole−dipole polarizability. $\alpha_{\alpha\beta}$ is defined through the following sum over the system's states

$$\alpha_{\alpha\beta} = \sum_{n\neq 0}^{\infty} \frac{\langle 0|\hat{\mu}_\alpha|n\rangle\langle n|\hat{\mu}_\beta|0\rangle + \langle 0|\hat{\mu}_\beta|n\rangle\langle n|\hat{\mu}_\alpha|0\rangle}{E_n - E_0} \tag{2}$$

In some cases, higher-order static multipoles and polarizabilities can also play an important role. For example, it has been suggested that specific features of the SFG spectra of the benzene−air interface can be associated with both quadrupole moment and dipole−quadrupole polarizabilities.[12] However, this appears not to apply to water for which only the dipole and dipole−dipole polarizabilities effectively contribute to eq 1. For this reason, in the following, the focus will be on the many-body convergence of μ_α and $\alpha_{\alpha\beta}$ of water, and, for the sake of simplicity, the dipole−dipole polarizability will be simply referred to as the polarizability.

Any total property p^T of an N-molecule system can be formally broken down into a many-body expansion

$$p^T_{\alpha\beta\ldots\omega}(1, \ldots, N) = \sum_i^N p^{1B}_{\alpha\beta\ldots\omega}(i) + \sum_{i<j}^N p^{2B}_{\alpha\beta\ldots\omega}(i, j) + \ldots \tag{3}$$

where p^{1B}, p^{2B}, ..., refer to the one-body, two-body, ..., contributions, respectively. The 1B term is defined by the

Received: August 5, 2013
Published: September 16, 2013

   dx.doi.org/10.1021/ct400696d | J. Chem. Theory Comput. 2013, 9, 4844−4852

nuclear coordinates of a single monomer (which are collectively defined here by a single index, e.g., "i"). The 2B contribution depends on the nuclear coordinates of the dimer comprising monomers "i" and "j", with the greek subscripts $\alpha\beta$ ...ω representing the Cartesian components. In the case of tensor properties, such as μ_α and $\alpha_{\alpha\beta}$, any component of p^T is obtained by summing over the corresponding composite interactions.

In the following, the 1B dipole and polarizability are defined as the corresponding monomer quantities,

$$\mu_\alpha^{1B}(i) = \mu_\alpha(i)$$

$$\alpha_{\alpha\beta}^{1B}(i) = \alpha_{\alpha\beta}(i)$$

All higher-order terms are defined recursively through eq 3. For example, the 2B dipole term is obtained by subtracting the 1B contributions from the dimer dipole

$$\mu_\alpha^{2B}(1, 2) = \mu_\alpha(1, 2) - \sum_i^2 \mu_\alpha^{1B}(i) \tag{4}$$

and the 3B contribution is calculated by subtracting all 1B and 2B terms from the trimer dipole

$$\mu_\alpha^{3B}(1, 2, 3) = \mu_\alpha(1, 2, 3) - \sum_{i<j}^3 \mu_\alpha^{2B}(i, j) - \sum_i^3 \mu_\alpha^{1B}(i) \tag{5}$$

Provided it converges relatively quickly, eq 3 thus represents a convenient framework for reconstructing the total dipole and polarizability of an N-molecule system from the sum of lower-order contributions. The many-body expansion has been employed in quantum mechanical models such as X-POL[13,14] and the effective fragment potential method.[15]

In this regard, it should be noted that a proper representation of polarizability and nonadditive effects may have important implications in the description of water in heterogeneous environments, such as interfaces[5] and confined environments.[6] Furthermore, water is characterized by a relatively large molecular polarizability and it has been demonstrated that nonadditive contributions to the total energy are non-negligible.[16−24] Therefore, it is expected that 2B and higher-order contributions can make a significant contribution to the total dipole moment of N-molecule systems. Perhaps less understood is how the polarizability of a gas-phase water molecule changes upon solvation. It has been suggested that promotion of electrons to some of the more-diffuse excited states appearing in eq 2 may be forbidden in the condensed phase because of the Pauli principle.[25,26] As a result, it is expected that only a subset of excited states in eq 2 are effectively allowed in the condensed phase, leading to a decrease of the molecular polarizability. In this context, it is interesting to consider how this restricted sum is manifest in water within a many-body expansion framework. If the polarizability is curtailed upon solvation, is it through the low-order (i.e., 2B and 3B) terms or through global N-body contributions that depend on the molecular configurations of the entire system?

While the total electrostatic properties of small clusters have been studied extensively, the associated many-body convergence has been explicitly examined only for a few systems. Early investigations focused on the 2B and 3B interaction-induced properties of noble gas trimers,[27−30] with higher-order effects being examined only for helium pentamers.[29] More recently, the many-body properties of hydrogen-bonded systems such as HF[31−34] and formaldehyde[34] chains have also been investigated. Though the specific details vary depending on the particular hydrogen-bonded system analyzed, these studies demonstrate that the higher-than-1B contributions to both dipole and polarizability are effectively dominated by 2B effects. It is important to note, however, that the dipole hyperpolarizability appears to have a more substantial contribution from the beyond-2B terms.[32,33]

For water, ab initio studies of the many-body convergence of dipole and polarizability are more scarce. Several studies have focused on the electrostatic properties of the water dimer.[35−37] The polarizability of larger water clusters has been examined, where it was found that the average monomer polarizability saturates quickly with cluster size.[38−41] In ref 42, it was speculated that the total dipole could reasonably be approximated by considering 1B and 2B contributions only. It was also shown that the total dipole of the prism isomer of the water hexamer is effectively dominated by low-order contributions.[43] By contrast, the many-body convergence of the interaction energy for water systems has been studied extensively.[16−24] In the case of the hexamer, it was found that 2B terms represent a large fraction of the total interaction energy, although 3B terms can contribute up to 30%. All higher-order interactions contribute less than 5%.[23] Estimates of the many-body convergence in the condensed phase through the decomposition of the 21-mer cluster into 1B−4B contributions were largely consistent with the conclusions derived from the hexamer studies.[21]

In this study, a systematic analysis of the convergence of the many-body expansion of the water dipole and polarizability is reported. As mentioned above, this is the first step toward the development of "first principles" theoretical approaches to vibrational spectroscopy. In section 2, the computational methods used to assess the convergence are discussed. Since the calculation of the many-body decomposition of the dipole and polarizability is computationally demanding, one of the goals of section 2 is to determine the accuracy of the electrostatic properties calculated with different electronic structure methods and basis sets. The many-body convergence is then studied in section 3 for small $(H_2O)_N$ clusters with N = 4−6 as well as for 14-mers extracted from classical simulations of liquid water and ice I_h. A summary highlighting the main findings and discussing future direction is given in section 4.

2. METHODS

2.1. Calculation of Electrostatic Properties through Finite Differences or Analytical Methods. Beginning with the expression describing the interaction of a single molecule with an electric field (eq 1), Kurtz et al.[44] obtained the following equations, which are used here for finite-field calculations of both μ_α and $\alpha_{\alpha\beta}$

$$\mu_\alpha = -\frac{1}{12F_\alpha}[8[E(F_\alpha) - E(-F_\alpha)] - [E(2F_\alpha) - E(-2F_\alpha)]] \tag{6}$$

$$\alpha_{\alpha\alpha} = \frac{1}{12F_\alpha^2}[30E(0) - 16[E(F_\alpha) + E(-F_\alpha)] + [E(2F_\alpha) + E(-2F_\alpha)]] \tag{7}$$

dx.doi.org/10.1021/ct400696d | J. Chem. Theory Comput. 2013, 9, 4844−4852

$$\alpha_{\alpha\beta} = \frac{1}{48F_\alpha F_\beta}[-16[E(F_\alpha, F_\beta) - E(F_\alpha, -F_\beta) - E(-F_\alpha, F_\beta) + E(-F_\alpha, -F_\beta)] + [E(2F_\alpha, 2F_\beta) - E(2F_\alpha, -2F_\beta) - E(-2F_\alpha, 2F_\beta) + E(-2F_\alpha, -2F_\beta)]] \quad (8)$$

All calculations were performed with Molpro (version 2012.1).[45] Fields of 0.005 au were used to ensure numerical stability, and the accuracy was validated with respect to the corresponding analytical calculations, which, however, are possible in Molpro only at the HF and MP2 levels.

2.2. Choice of Metrics for Many-Body Convergence. In contrast to the many-body expansion of the interaction energy, the convergence of eq 3 for both dipole and polarizability is somewhat more difficult to demonstrate. The symmetry of simple systems can be exploited to examine the variation of only one component of the dipole or polarizability (e.g., the longitudinal dipole and polarizability of linear chains of HF[31]) or to eliminate off-diagonal components in the polarizability tensor (e.g., the water dimer in C_{2v} symmetry[35]). However, one is often interested in the properties of structures that do not necessarily exhibit a well-defined symmetry (e.g., the global-minimum water dimer,[37] DNA base pairs,[46] and formaldehyde chains in the crystal structure configuration[33]). Since several approaches have been proposed in the literature, three different metrics are first discussed here in the context of the N-body decomposition of the dipole. In the simplest case, the N-body contribution to the total dipole, $\Delta\mu^N$, is defined as the ratio between the magnitude of the N-body term and the magnitude of the total dipole

$$\Delta\mu^N = \frac{\|\boldsymbol{\mu}^N\|}{\|\boldsymbol{\mu}^T\|} \quad (9)$$

This metric suffers from two main problems: (1) it is not normalized ($\sum_i \Delta\mu^{iB} \neq 1$) and (2) it does not provide any indication of how the many-body components combine to define the orientation of the dipole moment. These deficiencies can be partially addressed by comparing the magnitude of the sum of the many-body contributions up to order N with the total magnitude,

$$\varepsilon_\mu^N = \frac{\|\sum_{i=1}^N \boldsymbol{\mu}^{iB}\|}{\|\boldsymbol{\mu}^T\|} \quad (10)$$

To study the many-body convergence of a property measured through eq 10, differences between the N and $N-1$ terms are calculated with the exception of the 1B contribution, ε_p^1, which is simply given by

$$\Delta p^N = \begin{cases} \varepsilon_p^1 & N = 1 \\ \varepsilon_p^N - \varepsilon_p^{N-1} & N > 1 \end{cases} \quad (11)$$

Using this definition, it is evident that eq 10 is normalized with respect to the total dipole. Although eq 10 represents an improvement over eq 9, it can nonetheless be ambiguous because any term with incorrect direction but correct magnitude would have no error. To address this problem, a different quantity is considered in which the magnitude of the error vector $\boldsymbol{\mu}_{err}^N$ is compared to the magnitude of the total dipole

$$\boldsymbol{\mu}_{err}^N = \boldsymbol{\mu}^T - \sum_{i=1}^N \boldsymbol{\mu}^{iB} \quad (12)$$

$$\varepsilon_\mu^N = 1 - \frac{\|\boldsymbol{\mu}_{err}^N\|}{\|\boldsymbol{\mu}^T\|} \quad (13)$$

To guarantee a proper normalization, the many-body contributions of eq 13 are calculated through eq 11.

The 1B, 2B, 3B, and total dipole moments of the water trimer in the global minimum configuration are reported in the top half of Table 1, while the analysis of the relative contributions performed with the three metrics presented in eqs 9−13 is shown in the bottom half of the same table. Although eq 9 is not guaranteed to be normalized, in this case it correctly describes the relative contributions of 1B, 2B, and 3B terms. Since the 1B term has nearly the correct magnitude but the incorrect direction, eqs 10 and 11 erroneously predict the 2B dipole to have no contribution. The analysis of the Cartesian components of the many-body expansion reveals that the 2B contribution instead acts to mostly preserve the magnitude of the dipole while reorienting it, an effect that is correctly captured by eqs 13 and 11.

Table 1. Different Measures of the Many-Body Convergence of the Dipole[a]

dipole moment				
	1B	2B	3B	tot
x	0.036	−0.034	0.000	0.002
y	0.039	−0.001	−0.002	0.036
z	−0.970	−0.001	0.002	−0.969
many-body dipole contributions, $\Delta\mu^N$				
	1B	2B	3B	tot
eq 9	100.2%	3.5%	0.2%	104.0%
eq 10	100.2%	0.0%	−0.2%	100.0%
eq 13	96.5%	3.3%	0.2%	100.0%

[a]The structure examined is the global minimum water trimer at the BSSE-corrected CCSD(T)/d-aug-cc-pVTZ level. Dipoles are reported in Debye.

The rank-two tensor nature of the polarizability poses additional complications. The many-body convergence of the average diagonal elements has often been used in the literature

$$\alpha_{avg} = \frac{1}{3}[\alpha_{xx} + \alpha_{yy} + \alpha_{zz}] \quad (14)$$

However, for ($N > 1$)-body polarizabilities, the analysis in terms of the average polarizability can be somewhat ambiguous, as will be discussed below. Similarly to the dipole moment, the many-body convergence of the polarizability can also be studied through the magnitude of an error matrix

$$\boldsymbol{\alpha}_{err}^N = \boldsymbol{\alpha}^T - \sum_{i=1}^N \boldsymbol{\alpha}^{iB} \quad (15)$$

$$\varepsilon_\alpha^N = 1 - \frac{\|\boldsymbol{\alpha}_{err}^N\|_F}{\|\boldsymbol{\alpha}^T\|_F} \quad (16)$$

where $\|...\|_F$ indicates the Frobenius norm.

To investigate the proposed decrease in polarizability upon solvation, the convergence of the eigenvalues of the polarizability tensor is analyzed here for a few cases. For example, to

Table 2. Different measures of the many-body convergence of the polarizability. The structure examined is the global minimum water trimer at the BSSE-corrected CCSD(T)/d-aug-cc-pVTZ level. Polarizabilities are reported in Å^3

	1B Polarizbility			2B Polarizbility			3B Polarizbility		
	x	y	z	x	y	z	x	y	z
x	4.386	0.002	−0.001	0.197	0.002	0.027	−0.017	0.000	−0.004
y	0.002	4.372	−0.070	0.002	0.179	−0.113	0.000	−0.017	0.007
z	−0.001	−0.070	4.286	0.027	−0.113	−0.482	−0.004	0.007	0.012
α_{avg}		4.348/101.0%			−0.035/−0.8%			−0.007/−0.2%	
$\Delta\alpha_a^N$	96.4%	96.1%	112.5%	4.0%	4.3%	−12.9%	−0.4%	−0.4%	0.4%
$\Delta\alpha^N$		92.6%			7.0%			0.4%	

estimate the contribution of the 3B polarizability, the eigenvalues of the polarizability with up-to-3B terms ($\boldsymbol{\alpha}^{1B} + \boldsymbol{\alpha}^{2B} + \boldsymbol{\alpha}^{3B}$) can be calculated and normalized with respect to the eigenvalues of the total polarizability (eq 18)

$$\boldsymbol{\Lambda}(\boldsymbol{\alpha}^N) = \boldsymbol{V}^{-1}[\sum_{i=1}^{N} \boldsymbol{\alpha}^{iB}]\boldsymbol{V} \tag{17}$$

$$\varepsilon_{\alpha;a}^N = \frac{\boldsymbol{\Lambda}_{aa}(\boldsymbol{\alpha}^N)}{\boldsymbol{\Lambda}_{aa}(\boldsymbol{\alpha}^T)} \tag{18}$$

The contribution of the 3B polarizability is then given by applying eq 11 to each eigenvalue. Table 2 reports the results for the many-body convergence of the polarizability calculated for the global minimum energy configuration of the water trimer. This analysis clearly shows that focusing on the average polarizability may have several drawbacks. First, the components of the many-body polarizability tensors are signed and, therefore, can cancel one another when summed. For this reason, the 2B polarizability of the water trimer appears to be nearly negligible when measured through the average polarizability. By contrast, examination of the individual eigenvalues shows that the 2B term plays a significant role by acting to reorient the trimer polarizability. Importantly, although the net effect of the 2B terms is to decrease the monomer polarizabilities, the polarizability is actually enhanced along some directions. A second drawback is that the off-diagonal elements are neglected. Though the off-diagonal elements are often small relative to the diagonal 1B components; in the case of the 2B term, they can be as large as the diagonal ones. This underscores the need to calculate the full polarizability tensor when examining differences in polarizability tensors for systems where the off-diagonal elements are not zero by symmetry.

2.3. Basis-Set Superposition Error. As is well-known, the basis-set superposition error (BSSE) is an artifact associated with the incomplete nature of the basis functions that are used to calculate intermolecular interactions.[47] The most commonly used correction to this problem is the Boys−Bernardi counterpoise (CP) method.[47] The CP method was extended to the calculation of higher-order many-body interactions through the "site−site" function counterpoise (SSFC) method, which requires the N-body and lower-order interactions to be calculated in the basis-set of the N-mer system.[27] The SSFC method is advantageous in that its many-body contributions can be directly summed to give the energy of the whole N-molecule system. To achieve this, however, the SSFC method causes the $M < N$-body interactions to depend on the basis set of the complete N-mer (except at the complete basis set limit). A different approach to the many-body BSSE correction is the Valiron−Mayer function counterpoise (VMFC) method.[48,49] VMFC addresses the SSFC dependence on the N-mer basis set through the calculation of the 1B interaction in the monomer basis, the 2B interaction in the dimer basis, etc.

Since both dipole and polarizability are calculated through partial derivatives of the energy with respect to external electric fields, the electrostatic properties discussed here intrinsically suffer from BSSE. For most calculations presented in this study, the SSFC method is used to correct for BSSE. For larger systems, (i.e., the water 14-mers discussed in Section 3), it is not feasible to perform the many-body decomposition using the full cluster basis set, and, therefore, the VMFC method is used. Because the VMFC method lacks a simple relation to the total cluster energy, the convergence of the many-body expansion can in principle be established only after computing the full many-body decomposition (up to 14B interactions).

As this is clearly impractical, the effect of approximating the true VMFC correction with the sum of 1B through 3B contributions [VMFC(3B)] is studied in Table 3 using the

Table 3. Many-body percent contributions for the prism hexamer properties using different BSSE correction schemes. To make comparison with the 14-mer calculations presented later, these calculations are performed at RI-MP2/aug-cc-pVDZ. See Section 2.3 for details

	Dipole			Polarizability		
	1B	2B	3B	1B	2B	3B
SSFC	90.3	7.4	2.1	95.0	4.0	0.9
VMFC	90.2	7.6	2.1	94.7	4.2	0.9
VMFC(3B)	90.3	7.6	2.2	94.8	4.2	0.9
VMFC(SMol)	90.7	6.7	2.1	97.0	−1.5	−0.7

(smaller) water hexamer at the RI-MP2/aug-cc-pVDZ level. The VMFC(3B) many-body contributions are in good agreement with the true VMFC contributions as well as the SSFC results. This indicates that 1B-3B terms effectively dominate the dipole and polarizability of water independently of the system size. This analysis also demonstrates that it is inappropriate to compare the VMFC many-body contributions to the total supermolecular cluster calculation [VMFC(SMol)]. Since a consistent application of either SSFC or VMFC requires a significant amount of computational resources and considering that VMFC(3B) provides comparable accuracy, it thus appears reasonable to apply the VMFC(3B) method to the study of the 14-mer cluster.

2.4. Treatment of electronic correlation and the basis set. The dependence of the many-body dipole and polarizability on the electron correlation was investigated using three different methods: HF, MP2, and CCSD(T).[50,51] Dunning's correlation consistent basis sets, cc-pVXZ, with X = D, T, Q, and 5, were used in the calculations.[52] Because an accurate determination of the polarizability requires diffuse basis

dx.doi.org/10.1021/ct400696d | J. Chem. Theory Comput. 2013, 9, 4844−4852

functions,[53] augmented (aug-) and double augmented (d-aug-) functions[54,55] were added to the cc-pVXZ basis sets. Unless otherwise stated, all calculations were corrected for BSSE using the SSFC method as described previously. Note that all calculations presented in this article use flexible monomer geometries.

In Figure 1, the convergence of the total dipole and polarizability of the global minimum energy configuration of

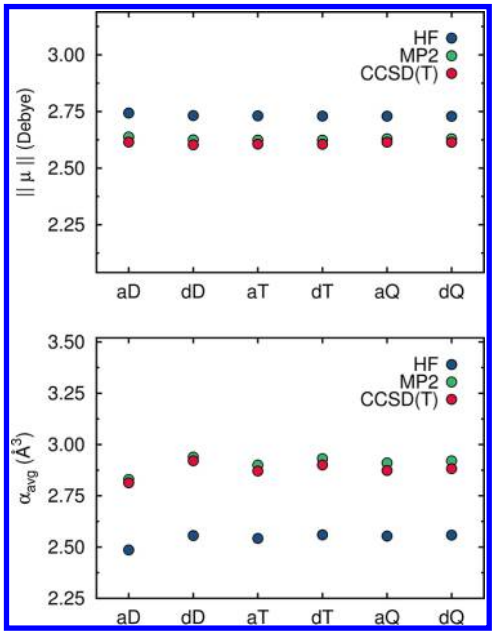

Figure 1. Dipole magnitude and average polarizability for the dimer global minimum structure as a function of basis set/method. In the basis set abbreviations on the *x*-axis, the lower-case letter refers to the size of the diffuse basis (a is "aug-" and d is "d-aug-") and the capital letter refers to the cardinal number from the cc-pVXZ basis set (X ∈ {D,T,Q,5,}). For example, dD is the d-aug-cc-pVDZ basis set. To compare the dipole and polarizability, the range of the *y*-axes are normalized to a 25% deviation from the CCSD(T)/dQ value. The values plotted in this figure are available in the Supporting Information for further inspection.

the water dimer is presented as a function of the basis set for HF, MP2, and CCSD(T). This analysis clearly show that the treatment of correlation effects is the primary source of error. In addition, as expected, the polarizability is more sensitive to the basis-set size than the corresponding dipole. To test the dependence of the decomposition of the dipole and polarizability 1B and 2B terms on the basis set and method, the many-body contributions of the water dimer global minimum geometry are presented in Figure 2. The basis-set convergence of the 3B dipole and polarizability is studied using the results obtained for the global minimum energy configuration of the water trimer in Figure 3. The basis set convergence is studied using

$$\sigma(\boldsymbol{p}^N) = \frac{\|\boldsymbol{p}^{NB}_{\text{ref}} - \boldsymbol{p}^{NB}_{\text{method}}\|}{\|\boldsymbol{p}^{T}_{\text{ref}}\|} \tag{19}$$

where p indicates the electrostatic property. These values, plotted in Figure 2 and Figure 3, can be interpreted as the relative error that a given N-body term contributes to the total property. Partially because both dipole and polarizability are dominated by the 1-body interactions (see Section 3), correlation effects and basis set truncation artifacts most significantly impact the total values at the 1B level. Similarly to the results shown in Figure 1, the accuracy is primarily limited by the treatment of the electronic correlation, although the error associated with basis-set truncation can contribute up to 2.5%.

At the 1B level, the difference between the HF and CCSD(T) results may be as large as 8% for the dipole and 12% for the polarizability. At the 2B level on the other hand, the post-HF correlation accounts for only 1% of the dipole and 2.5% of the polarizability. MP2 recovers much of the correlation effects at the 1B and 2B levels, falling within 0.1−1% and 0.7−2% of the CCSD(T) results for the dipole and polarizability, respectively. Correlation and finite-size basis set effects are much smaller at the 3B level, which is consistent with observations made about the 3B interaction energy.[23] Note that because the many-body expansion used here is defined by the cluster's (clamped) nuclear coordinates, our analysis includes the monomer distortion effects in the 1B term. In all cases studied, correcting for BSSE almost always improves the agreement of the specific property relative to the converged basis-set result for a particular method. As the polarizability is more sensitive to the basis-set size, it also exhibits larger BSSE than the dipole for a given method/basis. For basis sets larger than aug-cc-pVQZ, however, the BSSE becomes negligible.

3. MANY-BODY DECOMPOSITION OF THE DIPOLE AND THE POLARIZABILITY OF WATER CLUSTERS

The many-body decomposition of both the dipole and the polarizability of small $(H_2O)_N$ clusters with N = 4−6 is presented in Tables 4 and 5, respectively. The clusters, arranged from top to bottom in order of increasing binding energy, are obtained from refs 56 and 57. As is well-known, the lowest energy isomers of the 4-mer and 5-mer are cyclic, with all oxygen atoms lying in the same plane. The hexamer is the smallest water cluster whose minimum-energy configuration has a three-dimensional hydrogen-bond network. Because the hexamer has several nearly iso-energetic yet topologically distinct isomers, characterizing the properties of the hexamer in particular has long been of interest to both theorists[23,57−60] and experimentalists.[61−65] On the basis of the results presented in Figures 2 and 3, all calculations for these clusters were performed at the BSSE-corrected RI-MP2/aug-cc-pVTZ level.[66,67] RI-MP2 was found to agree with MP2 to within 10^{-6} a.u. for the dipole and 10^{-3} a.u. for the polarizability.

The many-body decomposition of the small cluster dipoles is presented in Table 4. The dipole moments of the S_4 and C_i 4-mer and the cyclic hexamer are zero by symmetry. For nearly all clusters, the permanent dipole of the noninteracting water monomers in the cluster configuration comprises more than 80% of the total dipole. Surprisingly, to a good approximation, the dipole for these clusters is largely pairwise additive. While 3B interaction energies can constitute up to 30% of the interaction energy for these clusters, nonadditive induced dipole effects account only for <2.5% of the total dipole. Similarly to the dipole, the many-body decomposition of the polarizability is dominated by the 1B term. As shown in Table 5, the 2B polarizability contributes up to 9%, while the 3B term is responsible for roughly 1%. For both dipole and polarizability, 4B and higher contributions give rise to at most 0.2% to the total property.

In an attempt to assess the convergence of eq 3 for condensed phase water systems, the global minimum energy

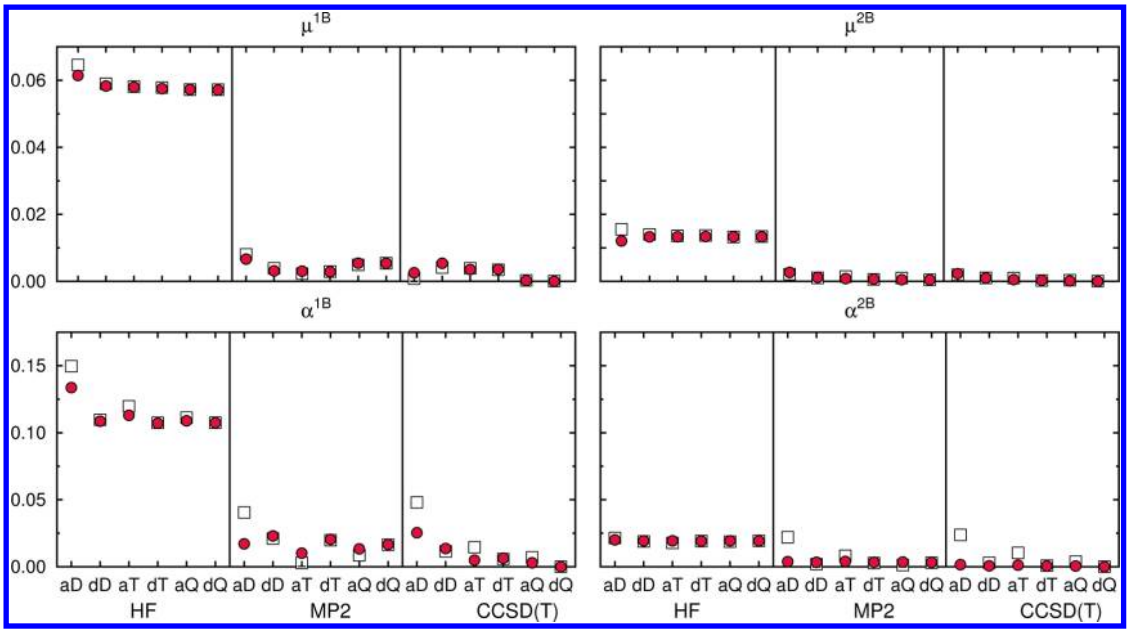

Figure 2. Basis set dependence of the decomposition of the total dipole and polarizability for the global minimum dimer into 1B and 2B contributions. On the *x*-axis is the method/basis. The basis set abbreviations are as described in Figure 1. On the *y*-axis, the magnitude of the differences between each method/basis and the CCSD(T)/d-aug-cc-pVQZ values are presented with respect to the magnitude of the total property (see eq 19). BSSE-corrected values (using SSFC) are plotted with solid circles, uncorrected values with open squares. The values plotted in this figure are available in the Supporting Information for further inspection.

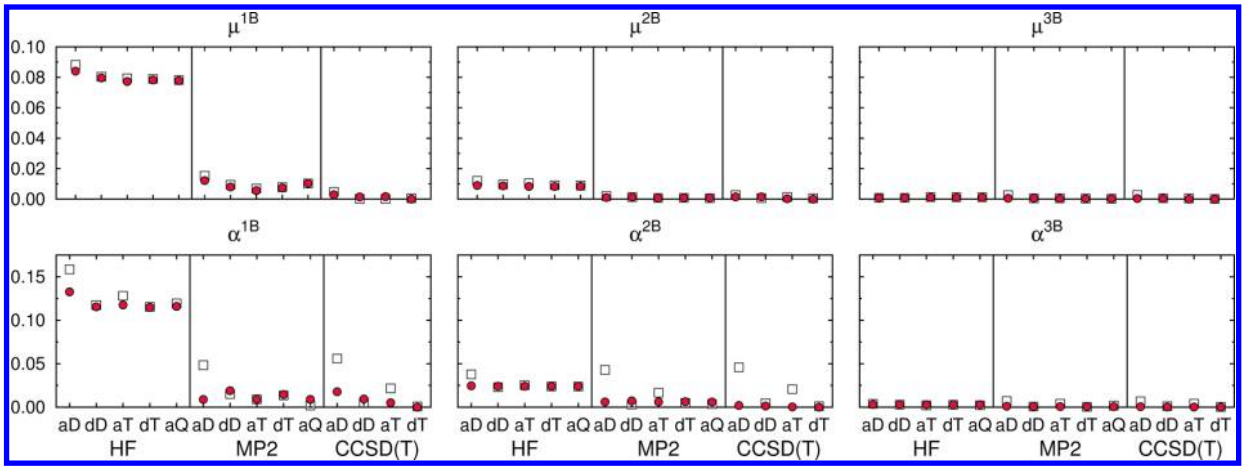

Figure 3. Basis set dependence of the decomposition of the total dipole and polarizability for the global minimum trimer into 1B, 2B, and 3B contributions. The values on the *y*-axis are relative to CCSD(T)/d-aug-cc-pVTZ. The values plotted in this figure are available in the Supporting Information for further inspection. See the caption of Figure 2 for a more detailed description.

configuration of the 14-mer cluster (as recently determined Kazachenko and Thakkar[68] using the Amoeba force field[69]) is also analyzed along with four 14-mer clusters that were randomly extracted from 100 ps classical molecular dynamics simulations of liquid water at ambient density at 298 K and ice I_h at 50 K using the HBB2-pol[70,71] and TTM3-F[72] potentials, respectively. The liquid and ice 14-mer configurations can be found in the Supporting Information of this paper, while the configuration of the AMOEBA 14-mer global minimum structure can be found in the Supporting Information of ref 68. The 14-mer clusters were specifically chosen because they are large enough to contain at least one molecule that is completely "solvated" by the remaining molecules yet of sufficiently small size that the many-body decomposition of both dipole and polarizability is still feasible. As discussed in section 2.3, since the SSFC method becomes prohibitively expensive for large clusters, the VMFC(3B) method was used to correct for BSSE in all calculations of the 14-mer clusters that were carried out at the RI-MP2/aug-cc-pVDZ level.

The many-body convergence of the polarizability is consistent between small clusters and 14-mers, with the 1B term contributing more than 90%, the 2B term 2−5%, and 3B less than 2.5%. For the many-body convergence of the dipole, the contributions of the 1B and 2B dipoles are in competition. This behavior, which is distinct from that of the polarizability, originates in part from the fact that, while the 1B polarizability eigenvalues are always large and positive, the 1B dipole moments can combine constructively or destructively, depending on their orientation. The extent to which the many-body dipoles constructively or destructively interfere can be determined by the difference between the orientation-independent (eq 10) and orientation-dependent (eq 13)

dx.doi.org/10.1021/ct400696d | J. Chem. Theory Comput. 2013, 9, 4844−4852

Table 4. Percent Contribution of the Many-Body Dipoles to the Total Cluster Dipole, Computed at the RI-MP2/aug-cc-pVTZ Level[a]

			dipole			
	isomer	C/D	1B	2B	3B	4B
4-mer	S_4					
	C_i					
	pyramid	D(4%)	96.4	2.5	1.1	0.0
5-mer	cyclic	D(6%)	95.4	4.1	0.4	0.1
	FR-B	D(7%)	93.7	5.0	1.1	0.1
	cage-C	C	96.1	2.1	1.8	0.1
	cage-A	C	96.4	2.0	1.4	0.2
	cage-B	C	92.4	6.1	1.2	0.1
	FR-C	D(4%)	95.1	3.7	1.8	0.1
	FR-A	D(4%)	97.4	1.4	1.2	0.0
6-mer	prism	D(4%)	90.3	7.4	2.2	0.0
	cage	D(8%)	84.8	13.1	1.9	0.1
	book	D(5%)	90.5	6.7	2.4	0.3
	cyclic					

[a]BSSE was corrected through the SSFC method. All greater-than-4B dipoles are less than 0.1%. C/D refers to constructive or destructive interference of the dipoles, with the percentage being the difference between the orientation independent and dependent measures (eqs 10 and 13, respectively) .

Table 5. Percent Contribution of the Many-Body Polarizabilities to the Total Cluster Polarizability, Computed at the RI-MP2/aug-cc-pVTZ Level[a]

		polarizability			
	isomer	1B	2B	3B	4B
4-mer	S_4	91.1	8.0	0.7	0.2
	C_i	90.9	8.3	0.7	0.1
	pyramid	96.7	2.8	0.5	0.0
5-mer	cyclic	90.6	8.4	0.8	0.1
	FR-B	92.4	6.7	0.8	0.1
	cage-C	95.0	4.1	0.7	0.1
	cage-A	94.9	4.4	0.7	0.1
	cage-B	95.2	3.8	0.9	0.1
	FR-C	94.2	4.9	0.7	0.2
	FR-A	93.0	6.2	0.7	0.2
6-mer	prism	95.1	3.8	1.0	0.1
	cage	93.5	5.5	0.9	0.1
	book	92.6	6.2	1.0	0.1
	cyclic	91.0	8.1	0.8	0.1

[a]BSSE was corrected through the SSFC method. All greater-than-4B polarizabilities are less than 0.1%.

convergence metrics. When the difference is zero, the many-body dipoles are adding constructively; otherwise, the many-body dipoles are destructively interfering with one another. This effect is presented in Tables 4 and 6 where the threshold for interference to be considered destructive is taken as 3%.

Although the global minimum configuration of the 14-mer clusters (as predicted by the Amoeba force field[69]) has dipole contributions that are similar to those obtained for the smaller cluster minima, the broken hydrogen-bond configurations extracted from liquid and ice simulations exhibit different behavior. For these condensed phase configurations, it is seen that even when the 1B and 2B terms add constructively, the 2B term can still contribute substantially. Interestingly, while the many-body dipoles often destructively interfere to a small

Table 6. Many-Body Contributions to 14-mer Dipoles and Polarizabilities[a]

		dipole			polarizability		
isomer	C/D	1B	2B	3B	1B	2B	3B
liquid 1	C	62.6	35.6	1.7	96.7	1.8	1.5
liquid 2	D(6%)	82.2	14.7	3.0	95.4	3.1	1.5
ice 1	D(28%)	46.3	51.1	2.7	96.2	3.0	0.9
ice 2	C	65.7	33.0	1.3	96.1	2.8	1.2
global min[68]	D(7%)	90.1	6.0	3.9	93.4	4.3	2.2

[a]Calculations are performed at the RI-MP2/aug-cc-pVDZ level and corrected for BSSE using the VMFC(3B) method. The global minimum configuration is from an extensive study of the AMOEBA potential energy surface[68].

extent, in the case of the ice1 configuration the 2B term acts to reorient the 1B contribution to such an extent that the interaction-induced 2B dipole actually overcomes the monomer contribution. By contrast, the 3B dipoles make minor contributions in all cases, which is likely related in part to the rapid convergence of the many-body polarizability.

4. SUMMARY

The convergence of the many-body expansion of the dipole and the (dipole−dipole) polarizability for water was examined. It was demonstrated that methods commonly used to assess the many-body convergence of these two properties can often provide ambiguous results, especially for systems of lower symmetry. Alternative measures were introduced and used to study the dependence of both dipole and polarizability on electronic structure methods, basis sets, and schemes for correcting for the basis-set superposition error. It was found that, although the average diagonal polarizability elements associated with the 2B and 3B terms appear to slightly decrease relative to the gas-phase (1B) term, an analysis of the many-body convergence based on this observation may be incomplete. By considering the convergence of the eigenvalues individually, it was observed that the 2B polarizability can play a significant role, with water systems often becoming more polarizable in some directions relative to an isolated molecule.

The many-body convergence of both dipole and polarizability of $(H_2O)_N$ clusters with N = 4−6, 14 was also examined. It was shown that if the total dipole and polarizability of these clusters are treated as pairwise additive, more than 97.5% of the total value is recovered. The dipole and polarizability become accurate to within 99.8% if 3B terms are also included. This analysis suggests that a theoretical/computational strategy based on the many-body expansion of the electrostatic properties can be used to accurately determine the dipole and polarizability of condensed-phase water systems from highly correlated electronic structure calculations, as already done for the total interaction energy.[42,71,73,74] This, in turn, will enable the calculation of (linear and nonlinear) water vibrational spectra entirely from "first principles". Studies along these directions are ongoing.

■ ASSOCIATED CONTENT

Supporting Information

Values plotted in Figures 1−3 are available for further examination. Images of the 14-mer configurations used in this study, along with Cartesian coordinates for those clusters. This material is available free of charge via the Internet at http://pubs.acs.org/.

AUTHOR INFORMATION

Corresponding Author

*E-mail: fpaesani@ucsd.edu.

Notes

The authors declare no competing financial interest.

ACKNOWLEDGMENTS

This research was supported by the National Science Foundation through grant CHE-1111364. We are grateful to the National Science Foundation for a generous allocation of computing time on Xsede resources (award TG-CHE110009). Additionally, we would like to thank Volodymyr Babin and Greg Schenter for their valuable discussions and critical feedback in preparation of this manuscript.

REFERENCES

(1) Chaplin, M. *Nature Rev. Mol. Cell Bio.* **2006**, *7*, 861−866.
(2) Ball, P. *Chem. Rev.* **2008**, *108*, 74−108.
(3) Dash, J. G.; Fu, H.; Wettlaufer, J. S. *Rep. Prog. Phys.* **1995**, *58*, 115−167.
(4) Jubb, A. M.; Hua, W.; Allen, H. C. *Annu. Rev. Phys. Chem.* **2012**, *63*, 107−130.
(5) Jungwirth, P.; Winter, B. *Annu. Rev. Phys. Chem.* **2008**, *59*, 343−366.
(6) Rasaiah, J. C.; Garde, S.; Hummer, G. *Annu. Rev. Phys. Chem.* **2008**, *59*, 713−740.
(7) Ricci, M. A.; Bruni, F.; Gallo, P.; Rovere, M.; Soper, A. K. *J. Phys.: Condens. Matter* **2000**, *12*, A345−A350.
(8) Cirera, J.; Sung, J.; Howland, P. B.; Paesani, F. *J. Chem. Phys.* **2012**, *137*, 054704.
(9) Maréchal, Y. *The Hydrogen Bond and the Water Molecule: The Physics and Chemistry of Water, Aqueous and Bio-Media*; Elsevier: Amsterdam, 2006.
(10) Mukamel, S. *Principles of Nonlinear Optical Spectroscopy*; Oxford University Press: Oxford, 1995.
(11) Stone, A. J. *Theory of Intermolecular Forces*; Oxford University Press: Oxford, 1997.
(12) Matsuzaki, K.; Nihonyanagi, S.; Yamaguchi, S.; Nagata, T.; Tahara, T. *J. Phys. Chem. Lett.* **2013**, *4*, 1654−1658.
(13) Xie, W.; Gao, J. *J. Chem. Theory Comput.* **2007**, *3*, 1890−1900.
(14) Xie, W.; Song, L.; Truhlar, D. G.; Gao, J. *J. Chem. Phys.* **2008**, *128*, 234108.
(15) Gordon, M. S.; Slipchenko, L.; Li, H.; Jensen, J. H. *Annu. Rep. Comput. Chem.* **2007**, *3*, 177−193.
(16) Xantheas, S. S. *J. Chem. Phys.* **1994**, *100*, 7523−7534.
(17) Ojamie, L.; Hermansson, K. *J. Phys. Chem.* **1994**, *98*, 4271−4282.
(18) Pedulla, J. M.; Vila, F.; Jordan, K. D. *J. Chem. Phys.* **1996**, *105*, 11091.
(19) Hodges, M. P.; Stone, A. J.; Xantheas, S. S. *J. Phys. Chem. A* **1997**, *101*, 9163−9168.
(20) Xantheas, S. S. *Chem. Phys.* **2000**, *258*, 225−231.
(21) Cui, J.; Liu, H.; Jordan, K. D. *J. Phys. Chem. B* **2006**, *110*, 18872−18878.
(22) Hermann, A.; Krawczyk, R.; Lein, M.; Schwerdtfeger, P.; Hamilton, I.; Stewart, J. *Phys. Rev. A* **2007**, *76*, 013202.
(23) Góra, U.; Podeszwa, R.; Cencek, W.; Szalewicz, K. *J. Chem. Phys.* **2011**, *135*, 224102.
(24) Khaliullin, R. Z.; Cobar, E. A.; Lochan, R. C.; Bell, A. T.; Head-Gordon, M. *Phys. Chem. Chem. Phys.* **2012**, *14*, 15328−15339.
(25) Morita, A. *J. Comput. Chem.* **2002**, *23*, 1466−1471.
(26) Lamoureux, G.; Roux, B. *J. Phys. Chem. B* **2006**, *110*, 3308−3322.
(27) Wells, B. H.; Wilson, S. *Chem. Phys. Lett.* **1983**, *101*, 429−434.
(28) Perez, J. J.; Clarke, J. H. R.; Hinchliffe, A. *Chem. Phys. Lett.* **1984**, *104*, 583−586.
(29) Waite, J.; Papadopoulos, M. G. *Theor. Chem. Acta* **1989**, *75*, 53−65.
(30) Aleman, C.; Perez, J. J.; Hinchliffe, A. *Int. J. Mass Spectrom. Ion Process.* **1992**, *122*, 331−336.
(31) Skwara, B.; Bartkowiak, W.; Silva, D. L. *Theor. Chem. Acc.* **2009**, *122*, 127−136.
(32) Baranowska, A.; Zawada, A.; Fernández, B.; Bartkowiak, W.; Kedziera, D.; Kaczmarek-Kędziera, A. *Phys. Chem. Chem. Phys.* **2010**, *12*, 852−862.
(33) Zawada, A.; Bartkowiak, W. *Comput. Theor. Chem.* **2011**, *967*, 120−128.
(34) Zawada, A.; Kaczmarek-Kędziera, A.; Bartkowiak, W. *J. Mol. Model.* **2012**, *18*, 3073−3086.
(35) Karlstrom, G.; Sadlej, A. J. *Theor. Chem. Acta* **1982**, *61*, 1−9.
(36) Maroulis, G. *J. Chem. Phys.* **2000**, *113*, 1813−1820.
(37) Zawada, A.; Kaczmarek-Kędziera, A.; Bartkowiak, W. *Chem. Phys. Lett.* **2011**, *503*, 39−44.
(38) Ghanty, T. K.; Ghosh, S. K. *J. Chem. Phys.* **2003**, *118*, 8547−8550.
(39) Yang, M.; Senet, P.; Van Alsenoy, C. *Int. J. Quantum Chem.* **2005**, *101*, 535−542.
(40) Krishtal, A.; Senet, P.; Yang, M.; Van Alsenoy, C. *J. Chem. Phys.* **2006**, *125*, 034312.
(41) Hammond, J. R.; Govind, N.; Kowalski, K.; Autschbach, J.; Xantheas, S. S. *J. Chem. Phys.* **2009**, *131*, 214103.
(42) Wang, Y.; Huang, X.; Shepler, B. C.; Braams, B. J.; Bowman, J. M. *J. Chem. Phys.* **2011**, *134*, 094509.
(43) Wang, Y.; Shepler, B. C.; Braams, B. J.; Bowman, J. M. *J. Chem. Phys.* **2009**, *131*, 054511.
(44) Kurtz, H. A.; Stewart, J. J. P.; Dieter, K. M. *J. Comput. Chem.* **1990**, *11*, 82−87.
(45) Werner, H.-J.; Knowles, P. J.; Knizia, G.; Manby, F. R.; Schütz, M.; et al. *MOLPRO*, version 2012.1, a package of ab initio programs. 2012.
(46) Czyżnikowska, Z.; Góra, R.; Zaleśny, R.; Bartkowiak, W.; Baranowska-Łączkowska, A.; Leszczynski, J. *Chem. Phys. Lett.* **2013**, *555*, 230−234.
(47) Boys, S. F.; Bernardi, F. *Mol. Phys.* **1970**, *19*, 553.
(48) White, J. C.; Davidson, E. R. *J. Chem. Phys.* **1990**, *93*, 8029−8035.
(49) Valiron, P.; Mayer, I. *Chem. Phys. Lett.* **1997**, *275*, 46−55.
(50) Szabo, A.; Ostlund, N. S. *Modern Quantum Chemistry*; Dover Publications: Mineola, 1996.
(51) Raghavachari, K.; Truck, G. W.; Pople, J. A.; Head-Gordon, M. *Chem. Phys. Lett.* **1989**, *157*, 479−483.
(52) Dunning, T. H. *J. Chem. Phys.* **1989**, *90*, 1007.
(53) Roztoczyńska, A.; Kaczmarek-Kędziera, A.; Góra, R. W.; Bartkowiak, W. *Chem. Phys. Lett.* **2013**, *571*, 28−33.
(54) Kendall, R. A.; Dunning, T. H.; Harrison, R. J. *J. Chem. Phys.* **1992**, *96*, 6796−6806.
(55) Woon, D. E.; Dunning, T. H. *J. Chem. Phys.* **1994**, *100*, 2975−2988.
(56) Temelso, B.; Archer, K. A.; Shields, G. C. *J. Phys. Chem. A* **2011**, *115*, 12034−12046.
(57) Bates, D. M.; Tschumper, G. S. *J. Phys. Chem. A* **2009**, *113*, 3555−3559.
(58) Dahlke, E. E.; Olson, R. M.; Leverentz, H. R.; Truhlar, D. G. *J. Phys. Chem. A* **2008**, *112*, 3976−3984.
(59) Wang, Y.; Babin, V.; Bowman, J. M.; Paesani, F. *J. Am. Chem. Soc.* **2012**, *134*, 11116−11119.
(60) Foley, J. J.; Mazziotti, D. A. *J. Phys. Chem. A* **2013**, *117*, 6712−6716.
(61) Pribble, R. N.; Zwier, T. S. *Science* **1994**, *265*, 75−79.
(62) Liu, K.; Brown, M. G.; Carter, C.; Saykally, R. J.; Gregory, J. K.; Clary, D. C. *Nature* **1996**, *381*, 501−503.
(63) Nauta, K.; Miller, R. E. *Science* **2000**, *287*, 293−295.
(64) Steinbach, C.; Andersson, P.; Melzer, M.; Kazimirski, J. K.; Buck, U.; Buch, V. *Phys. Chem. Chem. Phys.* **2004**, *6*, 3320−3324.

(65) Perez, C.; Muckle, M. T.; Zaleski, D. P.; Seifert, N. A.; Temelso, B.; Shields, G. C.; Kisiel, Z.; Pate, B. H. *Science* **2012**, *336*, 897−901.
(66) Bernholdt, D. E.; Harrison, R. J. *Chem. Phys. Lett.* **1996**, *250*, 477−484.
(67) Feyereisen, M.; Fitzgerald, G.; Komomicki, A. *Chem. Phys. Lett.* **1993**, *208*, 359−363.
(68) Kazachenko, S.; Thakkar, A. J. *J. Chem. Phys.* **2013**, *138*, 194302.
(69) Ren, P.; Ponder, J. W. *J. Phys. Chem. B* **2003**, *107*, 5933−5947.
(70) Babin, V.; Medders, G. R.; Paesani, F. *J. Phys. Chem. Lett.* **2012**, *3*, 3765−3769.
(71) Medders, G. R.; Babin, V.; Paesani, F. *J. Chem. Theory Comput.* **2013**, *9*, 1103−1114.
(72) Fanourgakis, G. S.; Xantheas, S. S. *J. Chem. Phys.* **2008**, *128*, 074506.
(73) Bukowski, R.; Szalewicz, K.; Groenenboom, G. C.; van Der Avoird, A. *J. Chem. Phys.* **2008**, *128*, 094313.
(74) Bukowski, R.; Szalewicz, K.; Groenenboom, G. C.; van Der Avoird, A. *J. Chem. Phys.* **2008**, *128*, 094314.